Universität Hamburg
DER FORSCHUNG | DER LEHRE | DER BILDUNG

Heavy-Flavor Hadro-Production with Heavy-Quark Masses Renormalized in the $\overline{\mathrm{MS}}$, MSR and On-Shell Schemes

M.V. Garzelli, L. Kemmler, S. Moch, O. Zenaiev

Mostly from [arXiv:2009.07763]

II. Institute for Theoretical Physics - Hamburg

Fermion Masses and Renormalization Schemes

- Fermion Masses are fundamental parameters of the QCD Lagrangian.
- UV-divergences appearing in the HQ self-energies require renormalization.
- Renormalized self-energy Σ^R enters the full renormalized heavy-quark propagator D^R

$$D^R = \frac{i}{\not{p} - m - i\Sigma^R(p, m, \mu)} \tag{1}$$

$\rightarrow$ Fixing a renormalization scheme to find relation between bare and physical mass.

Pole-Scheme

- On-shell renormalization condition:

$$\Sigma(p^2 = m^2) = 0 \tag{2}$$

- Pole of the full quark propagator defines the pole mass at

$$p^2 = m^2 = (m^{\text{pole}})^2 \tag{3}$$

- independent of the renormalization scale μ_R and gauge invariant

→ Short comings: Pole-mass is based on the idea of quarks appearing as asymptotic states which is not true due to confinement.

  - renormalon ambiguity making m^{pole} carrying intrinsic uncertainties of order $\mathcal{O}(\Lambda_{QCD})$ (see Bigi et al. [hep-ph/9402360]) and Beneke, Braun [hep-ph/9402364])
  - poor convergence of perturbative series (see e.g. Dowling, Moch, Eur. Phys. J. C (2014) 74:3167)

→ Long distance (ld) sensitivity

Short-Distance Relation to the Pole Mass

Universität Hamburg
DER FORSCHUNG | DER LEHRE | DER BILDUNG

$$m^{\text{pole}} = m^{\text{sd}}(R, \mu_R) + \delta m^{\text{pole - sd}}(R, \mu_R) \tag{4}$$

- $\delta m^{\text{pole - sd}}$ removing the renormalon and the dependence of the sd-mass on ld-aspects
- sd-masses depend on two different scales: (see Hoang et al. [arXiv:0803.4214])

  μ_R: Renormalization scale connected to UV-divergences
  R: Scale associated with the IR-RGE

$\rightarrow$ Insensitivity of sd-masses to ld-aspects removes the renormalon ambiguity.

$\rightarrow$ Cross-section formulae become more complicated

$\overline{\text{MS}}$-Scheme

Universität Hamburg
DER FORSCHUNG | DER LEHRE | DER BILDUNG

- Subtraction of poles resulting from dimensional regularization.

$\rightarrow$ Mass becomes scale dependent.

- Renormalized mass evolves according to the RGE wrt. the renormalization scale μ_R, governed by the mass anomalous dimension $\gamma(\alpha_S(\mu_R))$ known up to four loops: (see Chetyrin, Steinhauser, [hep-ph/9907509] and [hep-ph/9911434] as well as Melnikov, Ritbergen, [hep-ph/9912391])

$$\mu_R^2 \frac{\mathrm{d}m(\mu_R)}{\mathrm{d}\mu_R^2} = -\gamma(\alpha_S(\mu_R))m(\mu_R) \tag{5}$$

- For $\overline{\text{MS}}$-scheme: $R = m(\mu_R)$

Mass-Conversion Pole- and $\overline{\text{MS}}$-Scheme

Universität Hamburg
DER FORSCHUNG | DER LEHRE | DER BILDUNG

- Well known conversion to the on-shell masses: (see e.g. Gray et al., Z. Phys. C48 (1990) 673-680)

$$m^{\text{Pole}} = m(\mu_R)\left(1 + \sum_{i=1}^{\infty} c_i \left(\frac{\alpha_S}{\pi}\right)^i\right) \tag{6}$$

- Coefficients c_i are scale dependent, $c_i \propto L = \ln\left(\frac{\mu_R^2}{m(\mu_R)^2}\right)$ and known up to four loops at present.
- Number of active flavours set to $n_f = n_{lf} + 1$
- For the $\overline{\text{MS}}$-mass renormalized at a specific scale $\mu_R = m(\mu_R)$, L terms cancel:

$$\begin{aligned} m^{\text{Pole}} = m(m)\Bigg\{&1 + 1.333\left(\frac{\alpha_S}{\pi}\right) + (13.44 - 1.041 n_{lf})\left(\frac{\alpha_S}{\pi}\right)^2 \\ &+ (190.595 - 27.0 n_{lf} + 0.653 n_{lf}^2)\left(\frac{\alpha_S}{\pi}\right)^3 + \mathcal{O}(\alpha_S^4)\Bigg\} \end{aligned} \tag{7}$$

MSR-Scheme

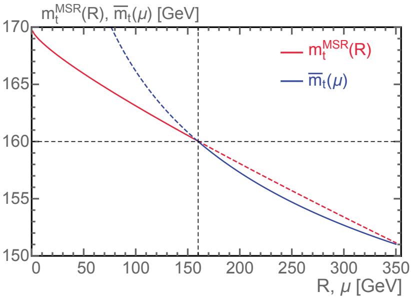

See Hoang et al., [arXiv:1704.01580].

$$m^{\text{MSR}}(R) \longrightarrow m^{\text{pole}}, \text{ for } R \longrightarrow 0$$
$$m^{\text{MSR}}(R) \longrightarrow m(m), \text{ for } R \longrightarrow m(m)$$

- Interpolation btw. pole- and $\overline{\text{MS}}$-scheme
- Pole- and MSR-mass at scale R differ by self-energy corrections (s.e.c.) from scales below R. (see Hoang et al., [arXiv:1704.01580])
    - Pole-mass absorbing all s.e.c. up to the scale of the HQ-mass
    - MSR-mass at scale R absorbs only s.e.c. between R and the HQ-mass

$\longrightarrow$ Pole-mass renormalon related to s.e.c. from the scale $\Lambda_{QCD} < R$.

$\longrightarrow$ MSR-mass is sd-mass.

Mass-Conversion Pole- and MSR-Scheme

- Consider difference btw. m^{pole} and (practical) m^{MSR}:

$$m^{\text{pole}} = m^{\text{MSR}}(R) + R \sum_{i=0}^{\infty} a_i \left(\frac{\alpha_S(R)}{\pi} \right)^i , \tag{8}$$

where coefficients a_i given in Hoang et al., [arXiv:0803.4214].

- Evolution of the MSR mass with the R scale follows the RGE: (see Hoang et al., [arXiv:1704.01580])

$$R \frac{\mathrm{d}m^{\text{MSR}}(R)}{\mathrm{d}R} = -R\gamma^{\text{MSR}}(\alpha_S(R)) \tag{9}$$

Diff. Cross-Sections in $\overline{\text{MS}}$- and MSR-Scheme

Universität Hamburg
DER FORSCHUNG | DER LEHRE | DER BILDUNG

1. Obtain cross sections with different mass renomalization schemes from the widely used on-shell prescription.
2. Substitute the pole-mass with its expressions in terms of the $\overline{\text{MS}}$- or MSR-mass (eq. (6) and (8)).
3. Perform a perturbative expansion in terms of α_S up to the needed order.

→ At NLO accurary, there is:

$$\sigma^{\overline{\text{MS}}}(m(\mu_R)) = \sigma^{\text{pole}}\Big|_{m^{\text{pole}}=m(\mu_R)} + (m(\mu_R) - m^{\text{pole}}) \left(\frac{\mathrm{d}\sigma^0}{\mathrm{d}m}\right)\Bigg|_{m=m(\mu_R)} \tag{10}$$

$$\sigma^{\text{MSR}}(m^{\text{MSR}}(R)) = \sigma^{\text{pole}}\Big|_{m^{\text{pole}}=m^{\text{MSR}}(R)} + (m^{\text{MSR}}(R) - m^{\text{pole}}) \left(\frac{\mathrm{d}\sigma^0}{\mathrm{d}m}\right)\Bigg|_{m=m^{\text{MSR}}(R)} \tag{11}$$

Diff. Cross-Sections for $t\bar{t}$-production

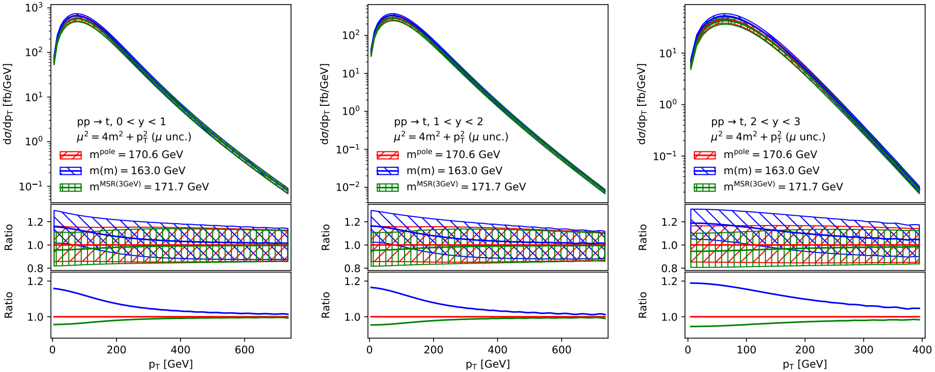

- top p_T distribution at NLO for the process $pp \longrightarrow t\bar{t}$ at $\sqrt{s} = 7$ TeV for various rapidity ranges
- Central prediction ($\mu_F = \mu_R$) at the peak sensitive to the choice of the renormalization scheme.
- ~ 20 % (~ 10 %) for comparing pole- and $\overline{\text{MS}}$ (MSR)-scheme
  - Impact not neglible when comparing to the NLO scale-uncertainties

PDF-Variation with a Dynamic Scale

Universität Hamburg
DER FORSCHUNG | DER LEHRE | DER BILDUNG

- $m_t(m_t) = 163$ GeV with $\mu_R = \mu_F = \sqrt{p_t^2 + 4m_t(m_t)^2}$
- Relatively small differences among predictions with different PDFs

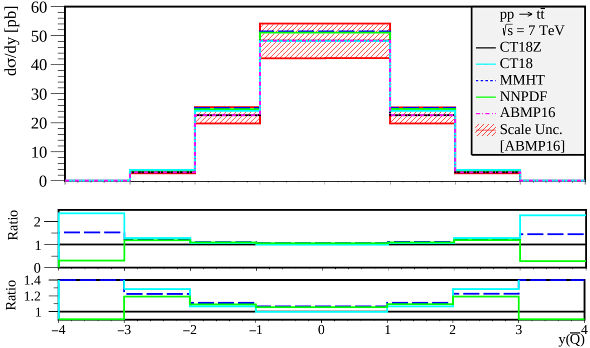

→ Predictions with different central PDFs still lay within the scale uncertainty band produced using the ABMP16 NLO nominal set.

Dynamical vs. Static Mass Ren. Scale

Universität Hamburg
DER FORSCHUNG | DER LEHRE | DER BILDUNG

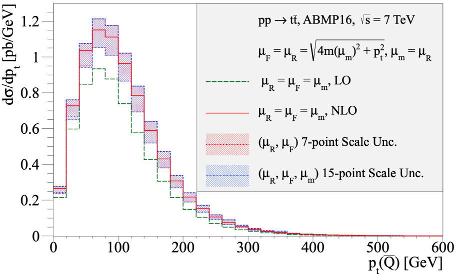

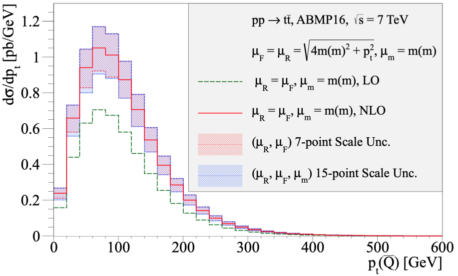

- 7-point variation: μ_m fixed; only (μ_R, μ_F) varied
- 15-point variation: (μ_R, μ_F, μ_m) varied independently
- $K = \frac{\sigma^{\mathrm{NLO}}}{\sigma^{\mathrm{LO}}}$: For the central predictions, we find for the total cross sections $K^{m(\mu)} = 1.3 < K^{m(m)} = 1.52$.

$\longrightarrow$ In the peak region ($\sim$ 70 GeV), $\Delta\sigma_{m(m)} =^{+14.4\,\%}_{-12.2\,\%}$ and $\Delta\sigma_{m(\mu)} =^{+5.3\,\%}_{-8.6\,\%}$.

$\longrightarrow$ Improved convergence and scale uncertainties using a dynamical mass renormalization scale.

$\longrightarrow$ Comparison consistent over the whole kinematic range.

Distributions with Various Scales

Universität Hamburg
DER FORSCHUNG | DER LEHRE | DER BILDUNG

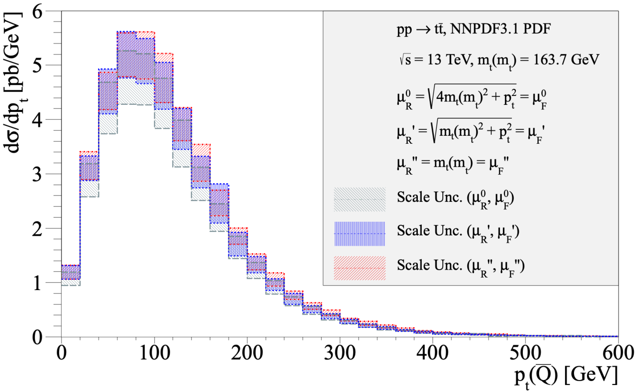

- Our NLO predictions consistent with those reported in (Catani et al., [arXiv:2005.00557]).
- Using (μ_R^0, μ_F^0) results in larger scale uncertainty bands than using (μ_R', μ_F') and (μ_R'', μ_F'').

Distributions with Various Scales

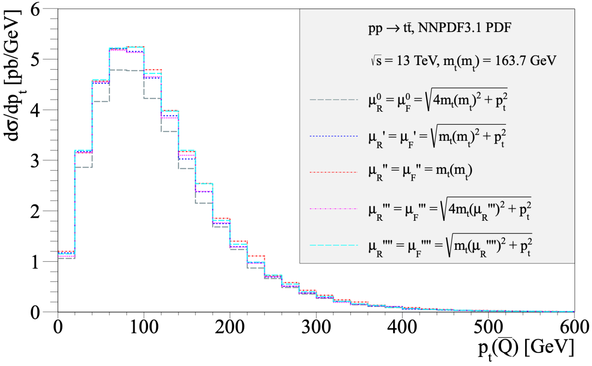

- Catani et al. reported small NNLO corrections for predictions with $\mu_R = \mu_F = m(m)$.
  (Catani et al., [arXiv:2005.00557])
- Predictions with μ_R''' lay close to μ_R' and μ_R''.
- Predictions with μ_R''' sit closer to $\mu_R'' = m(m)$ than those with μ_R^0

→ Slow perturbative convergence of μ_R^0 improved by using a dynamical mass renormalization scale instead of a static one.

Conclusions

- Sd-mass definitions have smaller parametric uncertainties compared to the pole mass definition.
- Choice of the mass scheme as well as the choice of μ_R, μ_F have impact on the rate of convergence of the perturbative expansion of the cross sections.
- Using a running mass, i.e. $m_t(\mu_m)$ evaluated at $\mu_m = \mu_R$, leads to reduced scale uncertainties and increased rate of convergence with respect to $m_t(m_t)$ for scales of the type $(\mu_R, \mu_F) = \sqrt{p_T^2 + \kappa m_t^2(\mu_m)}$ for $\kappa = 1 \ldots 4$.
- Analogous studies for charm and bottom were done as well as simultaneous extraction of α_S, m_t and PDFs in different mass renormalization schemes. (see our paper: [arXiv:2009.07763])

Thank you for your attention!

HQ MSR, $\overline{\text{MS}}$ and Pole Masses (in GeV)

Universität Hamburg
DER FORSCHUNG | DER LEHRE | DER BILDUNG

$m^{\text{MSR}}(1)$	$m^{\text{MSR}}(3)$ from $m(m)$	$m^{\text{MSR}}(9)$	$m(m)$	$m^{\text{pl}}_{\text{1lp}}$	$m^{\text{pl}}_{\text{2lp}}$ from $m(m)$	$m^{\text{pl}}_{\text{3lp}}$	$m^{\text{pl}}_{\text{1lp}}$	$m^{\text{pl}}_{\text{2lp}}$ from MSR(3)	$m^{\text{pl}}_{\text{3lp}}$
top-quark									
171.8	171.5	170.9	162.0	169.5	171.1	171.6	171.8	172.0	172.1
172.9	172.5	171.9	163.0	170.5	172.1	172.6	172.9	173.0	173.1
173.9	173.6	173.0	164.0	171.5	173.2	173.6	173.9	174.1	174.2
bottom-quark									
4.69	4.30	3.67	4.15	4.53	4.74	4.90	4.61	4.80	4.97
4.72	4.33	3.70	4.18	4.57	4.77	4.94	4.64	4.84	5.01
4.75	4.36	3.74	4.21	4.60	4.81	4.97	4.68	4.87	5.04
charm-quark									
1.33	0.94	0.31	1.25	1.46	1.68	1.98	1.25	1.44	1.61
1.37	0.97	0.35	1.28	1.50	1.70	2.00	1.29	1.48	1.65
1.40	1.01	0.38	1.31	1.53	1.73	2.02	1.33	1.52	1.69

- Input is $m(m)$. Fix $\alpha_S(M_Z)^{n_f=5} = 0.118$ and $\alpha_S(M_Z)^{n_f=3} = 0.106$ and α_S evolved at four loops in all cases.
- For top, MSR mass value at $R = 3$ GeV is numerically close to the values obtained in the on-shell scheme at two or three loops.
- Charm pole masses obtained from the conversion of $\overline{\text{MS}}$- or MSR-scheme do not seem to converge.

RGE Solutions providing HQ-Masses (1-Loop)

Universität Hamburg
DER FORSCHUNG | DER LEHRE | DER BILDUNG

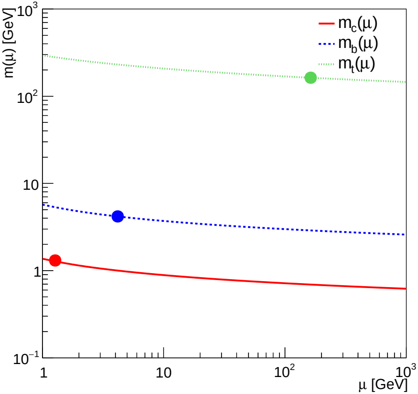

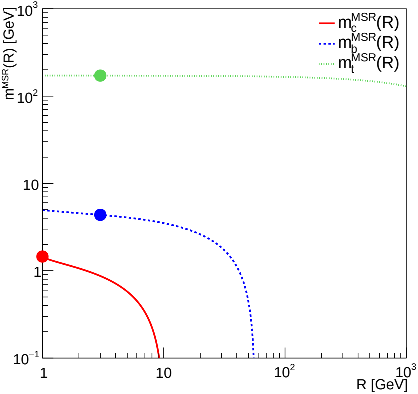

- RGE solutions providing HQ-masses at one-loop wrt. variations of the renormalisation scale (left) and the R-scale (right).
- Input: α_S evolution at four loops, with $\alpha_S(M_Z) = 0.118$ as reference value.

Differential Cross-Section wrt. $M_{t\bar{t}}$

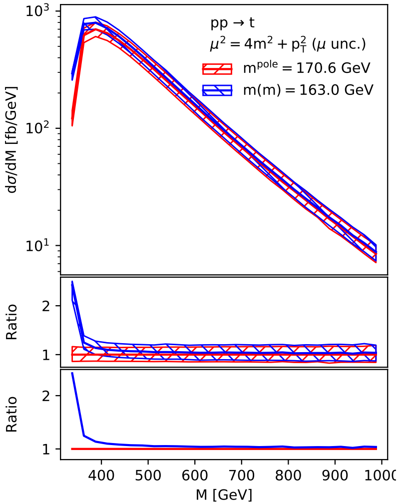

- No MSR-implementation for MCFM yet
- Impact of scheme choice largest at low $M_{t\bar{t}}$ close to production threshold due to derivative term in eq. (10) becoming dominant.

→ Exclusion of $\overline{\text{MS}}$-scheme from being a suitable mass renormalization scheme for observables close to threshold.

See Dowling, Moch, Eur. Phys. J. C (2014) 74:3167 for a detailed analysis of top-quark pair invariant mass distributions.

Dynamical vs. Static Mass Ren. Scale II

Universität Hamburg
DER FORSCHUNG | DER LEHRE | DER BILDUNG

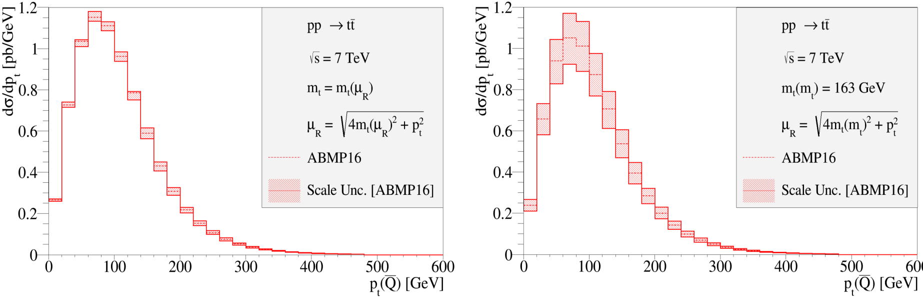

- 7-point scale variation with fixed μ_m: $\mu_m = \mu_R$ (left) and $\mu_m = m_t(m_t)$ (right).
- Scale uncertainties around the maximum ($\sim$ 70 GeV): $\Delta\sigma_{m(m)} =^{+11.3\ \%}_{-12.2\ \%}$ and $\Delta\sigma_{m(\mu)} =^{+5.3\ \%}_{-8.6\ \%}$.

$\longrightarrow$ Reduced scale uncertainties using a dynamical mass renormalization scale.

Total Cross-Sections HQs diff. Ren. Schemes

Universität Hamburg
DER FORSCHUNG | DER LEHRE | DER BILDUNG

Quark	$\sigma^{\mathrm{NLO}}_{\mathrm{Pole}}$	$\sigma^{\mathrm{NLO}}_{\overline{\mathrm{MS}}}$
charm	$3.97\,^{+65.5\%}_{-59.0\%}$ mb	$6.13\,^{+78.1\%}_{-69.6\%}$ mb
bottom	$0.23\,^{+36.9\%}_{-25.6\%}$ mb	$0.31\,^{+36.0\%}_{-26.9\%}$ mb
top	$0.12\,^{+15.6\%}_{-14.4\%}$ nb	$0.15\,^{+12.0\%}_{-12.5\%}$ nb

- Set up: MCFM, ABMP16 with 5 (3) flavours for top (charm, bottom).
- masses: $m_t^{\mathrm{Pole}} = 173$ GeV, $m_b^{\mathrm{Pole}} = 4.78$ GeV, $m_c^{\mathrm{Pole}} = 1.67$ GeV , $m_t(m_t) = 163$ GeV, $m_b(m_b) = 4.18$ GeV, $m_c(m_c) = 1.275$ GeV
- $\mu_r = \mu_F = \sqrt{4m_Q(m_Q)^2 + p_T^2}$

Extraction of Top Mass, $\alpha_s(M_Z)$ and PDFs

Universität Hamburg
DER FORSCHUNG | DER LEHRE | DER BILDUNG

Settings	Fit results
pole mass $\mu_R = \mu_F = H'$ Ref. CMS Coll.	$\chi^2/\mathrm{dof} = 1364/1151$, $\chi^2_{t\bar{t}}/\mathrm{dof} = 20/23$ $m_t^{\mathrm{pole}} = 170.5 \pm 0.7(\mathrm{fit}) \pm 0.1(\mathrm{mod})^{+0.0}_{-0.1}(\mathrm{par}) \pm 0.3(\mu)$ GeV $\alpha_S(M_Z) = 0.1135 \pm 0.0016(\mathrm{fit})^{+0.0002}_{-0.0004}(\mathrm{mod})^{+0.0008}_{-0.0001}(\mathrm{par})^{+0.0011}_{-0.0005}(\mu)$
pole mass $\mu_R = \mu_F = m_t^{\mathrm{pole}}$ this work	$\chi^2/\mathrm{dof} = 1363/1151$, $\chi^2_{t\bar{t}}/\mathrm{dof} = 19/23$ $m_t^{\mathrm{pole}} = 169.9 \pm 0.7(\mathrm{fit}) \pm 0.1(\mathrm{mod})^{+0.0}_{-0.0}(\mathrm{par})^{+0.3}_{-0.9}(\mu)$ GeV $\alpha_S(M_Z) = 0.1132 \pm 0.0016(\mathrm{fit})^{+0.0003}_{-0.0004}(\mathrm{mod})^{+0.0003}_{-0.0000}(\mathrm{par})^{+0.0016}_{-0.0008}(\mu)$
$\overline{\mathrm{MS}}$ mass $\mu_R = \mu_F = m_t(m_t)$ this work	$\chi^2/\mathrm{dof} = 1363/1151$, $\chi^2_{t\bar{t}}/\mathrm{dof} = 19/23$ $m_t(m_t) = 161.0 \pm 0.6(\mathrm{fit}) \pm 0.1(\mathrm{mod})^{+0.0}_{-0.0}(\mathrm{par})^{+0.4}_{-0.8}(\mu)$ GeV $\alpha_S(M_Z) = 0.1136 \pm 0.0016(\mathrm{fit})^{+0.0002}_{-0.0005}(\mathrm{mod})^{+0.0002}_{-0.0001}(\mathrm{par})^{+0.0015}_{-0.0009}(\mu)$
MSR mass, $R = 3$ GeV $\mu_R = \mu_F = m_t^{\mathrm{MSR}}$ this work	$\chi^2/\mathrm{dof} = 1363/1151$, $\chi^2_{t\bar{t}}/\mathrm{dof} = 19/23$ $m_t^{\mathrm{MSR}} = 169.6 \pm 0.7(\mathrm{fit}) \pm 0.1(\mathrm{mod})^{+0.0}_{-0.0}(\mathrm{par})^{+0.3}_{-0.9}(\mu)$ GeV $\alpha_S(M_Z) = 0.1132 \pm 0.0016(\mathrm{fit})^{+0.0003}_{-0.0004}(\mathrm{mod})^{+0.0002}_{-0.0000}(\mathrm{par})^{+0.0016}_{-0.0008}(\mu)$

- CMS data on double and triple differential cross sections reported in [arXiv:1904.05237] and H1-Zeus combined HERA inclusive DIS data [arXiv:1506.06042] used.
- Extraction procedure similar to the one used by the CMS collaboration. Extended for extractions of $\overline{\mathrm{MS}}$ and MSR top masses.

→ Results obtained in a *simultaneous* fit of $m_t(m_t)$, $\alpha_s(M_Z)$ and the PDFs preserving correlations among each other.

Comparisons for Different Mass Extractions

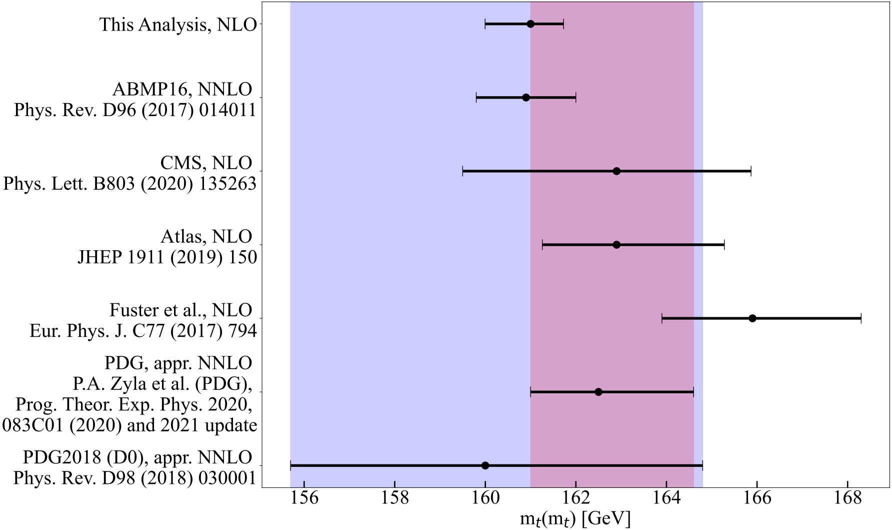

NNLO Differential Predictions

Universität Hamburg
DER FORSCHUNG | DER LEHRE | DER BILDUNG

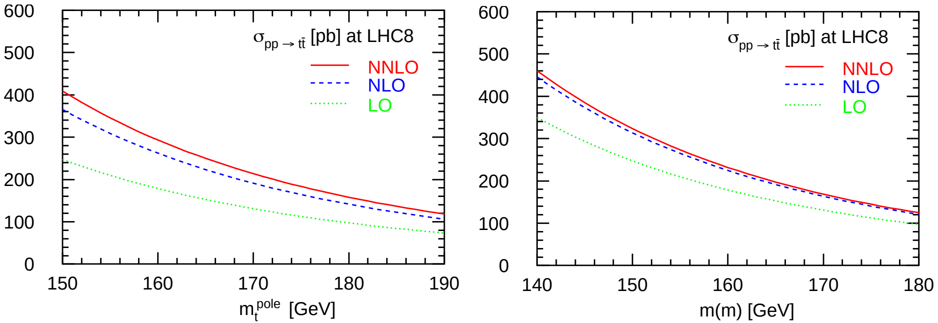

- $\sqrt{s} = 8$ TeV, $m_t^{\text{Pole}} = 173$ GeV, $m_t(m_t) = 163$ GeV, ABMP11
- $\mu = m_t^{\text{Pole}}$ (left), $\mu = m_t(m_t)$

$\rightarrow$ Relative increase in pole-scheme for $\mu_R = \mu_F = m_t^{\text{Pole}}$: $\frac{\sigma_{\text{NLO}}}{\sigma_{\text{LO}}} = 1.46$ and $\frac{\sigma_{\text{NNLO}}}{\sigma_{\text{NLO}}} = 1.12$.

$\rightarrow$ Relative increase in $\overline{\text{MS}}$-scheme for $\mu_R = \mu_F = m_t(m_t)$: $\frac{\sigma_{\text{NLO}}}{\sigma_{\text{LO}}} = 1.26$ and $\frac{\sigma_{\text{NNLO}}}{\sigma_{\text{NLO}}} = 1.03$.

See Dowling, Moch, Eur. Phys. J. C (2014) 74:3167.

NNLO Scale Uncertainties

Universität Hamburg
DER FORSCHUNG | DER LEHRE | DER BILDUNG

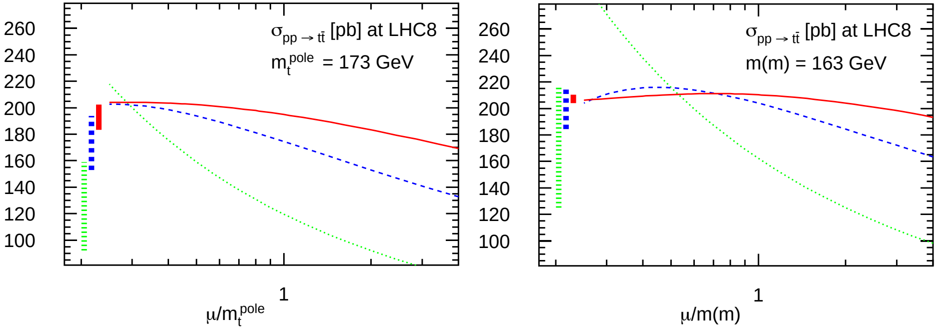

- $\sqrt{s} = 8$ TeV, ABMP11

$\rightarrow$ For the on-shell scheme, $\Delta\sigma_{\mathrm{NNLO}} = ^{+3.8\ \%}_{-6.0\ \%}$ for $\mu/m_t^{\mathrm{Pole}} \in [1/2, 2]$

$\rightarrow$ For the $\overline{\mathrm{MS}}$ scheme, $\Delta\sigma_{\mathrm{NNLO}} = ^{+0.1\ \%}_{-3.0\ \%}$

See Dowling, Moch, Eur. Phys. J. C (2014) 74:3167.

Diff. Distributions for $t\bar{t}H$

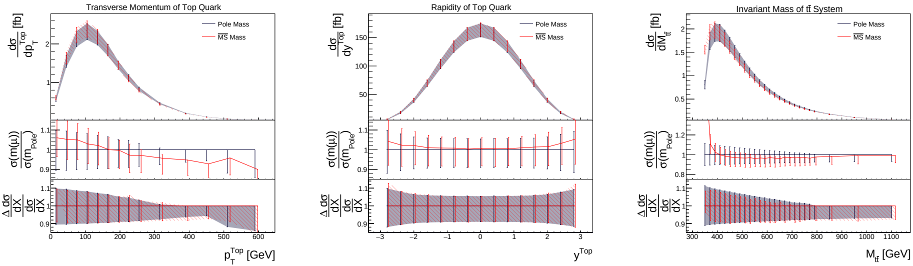

- Set up: MMHT2014 with $\alpha_S(M_Z) = 0.118$, $m_t(m_t) = 163.2$ GeV, $m_t^{\text{Pole}} = 172.5$ GeV, $m_H = 125$ GeV, $\mu_R = \mu_F = m_{t\bar{t}H}$

$\rightarrow$ Shape and scale uncertainties on cross sections show negligible differences between pole- and $\overline{\text{MS}}$-scheme.

See A. Saibel, *Phenomenology of $t\bar{t}H$ Production with Top Quark Running Mass and the Differential Cross-Section Measurement of $t\bar{t}$ + b-jets Production in the Dilepton Channel at $\sqrt{s}$ = 13 TeV with CMS Experiment*, PHD-Thesis, 2021.